International Journal of Marine Energy 19 (2017) 70–82

Contents lists available at ScienceDirect

International Journal of Marine Energy

journal homepage: www.elsevier.com/locate/ijome

Semi-analytical estimate of energy production from a tidal turbine farm with the account of ambient turbulence

Grégory Pinon *, Matías Fernández Hurst, Edile Lukeba

Normandie Univ, UNIHAVRE, CNRS, LOMC, 76600 Le Havre, France

ARTICLE INFO

Article history:
Received 27 July 2016
Revised 11 April 2017
Accepted 24 May 2017
Available online 1 June 2017

Keywords:
Tidal turbine
Interaction
Ambient turbulence
Power coefficient
Velocity deficit
Energy production

ABSTRACT

This paper presents the influence that ambient turbulence has on a tidal turbine farm. Firstly, the analytical model developed by Bahaj and Myers (2004) is used and modified in order to incorporate the ambient turbulence effects. Ambient turbulence is taken into account via the experiments of Mycek et al. (2014), where two levels of turbulences were tested, namely 3% and 15%. Modifications in wake velocity deficit are treated. However, the influence that ambient turbulence has on the power coefficient of downstream turbine(s), which is usually neglected, is taken into account. For the lower level of turbulence, three scenarios for the downstream turbine(s) behaviour are considered.

This enhanced model is then tested on a given site in the Alderney Race (Raz Blanchard). Yearly energy productions depending on ambient turbulence, turbine layouts and proposed scenarios are evaluated and compared. A technico-economical analysis is also carried out. Finally, the tidal turbine farm profitability highly depends on ambient turbulence and turbines layout.

1. Introduction

In 2004, Bahaj and Myers [3] published a paper performing an analytical estimate of tidal turbines farms in the Alderney Race. At the time, they evaluated the yearly energy production at 7.4 TWh. In the used methodology, they assumed twin-rotor turbines of different sizes arranged in several two-row farms. As a matter of turbine interaction between the two rows, it was assumed that the velocity deficit in the wake was negligible because the tidal turbines were disposed far enough from each other. However, a correction factor of 0.95 was applied to the downstream turbine to assume for power losses. Since this first work of the Southampton Sustainable Energy Research Group, several studies tried to improve the estimation of turbines interactions in a farm and also the influence that turbulence may have on a single turbine and on turbine interactions.

Numerically speaking, many authors computed turbines in a farm. For that purpose, several approaches were used from the more sophisticated blade resolved Computational Fluid Dynamics (CFD) to simpler and simpler model for the account of the turbine. With respect to more and more resolved CFD, O'Doherty et al. [34] performed some interesting computations using the 3D ANSYS-CFX model. Up to 3 turbines were computed with a blade resolved CFD. In the study, the turbines power coefficients were evaluated with a certain accuracy but the wake could not be enough resolved to assess turbines interactions. Similarly, Ahmed et al. [1] computed a turbine (including hub, nacelle and mast) in the LES and RANS approach with

* Corresponding author.
E-mail address: gregory.pinon@univ-lehavre.fr (G. Pinon).

http://dx.doi.org/10.1016/j.ijome.2017.05.003
2214-1669/

the EDF software *Code_Saturne*. The computations are impressive but the required CPU resources as well. And only a single turbine is considered without the resolution of the whole wake. Therefore, similar computations in a farm with several interacting turbines is still an challenge to the scientific community.

For these reasons of numerical complexity and the need of huge computational resources, many authors carried out research with simpler model for the turbine like the actuator-disk or -line coupled with CFD or regional models. For instance, one can cite the work of Divett et al. [10], who computed turbine interactions using the Gerris software with up to five rows of 3 turbines aligned with the flow direction. Roc et al. [39] used an actuator-disk appraoch and ROMS as a CFD model. Several others (Elie et al. [12] or Blackmore et al. [4,6], ...) also used an actuator-disk with many different CFD model. For instance, Karsten et al. [18] computed a farm with up to hundreds of turbines in the Bay of Fundy with a regional approach. Peyrard et al. [37] investigated the wake effects in farm using Telemac. Thiébot et al. [41] also computed farm in the Alderney Race with 2D and 3D versions of Telemac in the aim of hydro-sedimentary impact assessment.

A more sophisticated approach would be to use an actuator-line. Churchfield et al. [8] performed impressive LES computations for up to 5 turbines in a farm. The rotor were modelled by means of an actuator-line. Malki et al. [23] used a similar approach for three interacting turbines using the BEM + CFD method further developed recently [24,26,11]. Actuator-line or Blade Element Momentum (BEM) theory are supposed to be more accurate than a disk to model the rotor. However, one may wonder about the capability of such methods to capture and reproduce the complex flow that appends when rotors are aligned with the flow, as shown in some configurations tested by Churchfield et al. [8]. And what about turbulence, can it be taken into account? Togneri et al. [44] introduced the effect that ambient turbulence has on the calculation of power and thrust coefficients. Is this approach valid for large values of ambient turbulence? What is the real influence that ambient turbulence may have on turbines?

In the experimental field, Myers et al. [32] and Blackmore et al. [5] studied the influence of turbulence on a tidal turbine by means of porous disc, completed by some numerical computations [4,6]. Maganga et al. [22] performed a first study on turbulence influence on a single turbine completed recently by Mycek et al. [30]. More recently, Blackmore et al. [7] focused on turbulence influence on two different turbines in the IFREMER flume tank of Boulogne-sur-mer. Stallard et al. [40] studied wakes of several turbines, mostly regarding the wake recovery, lateral expansion or wakes merging for different lateral spacings and turbulence levels. Mycek et al. [28,29,31] studied interactions between two aligned turbines depending on turbulence and inter-device distances. From this last publication, Mycek et al. [31] showed that ambient turbulence largely modify the behaviour of a downstream turbine, in terms of power coefficient calculation with respect to the perceived velocity (see Fig. 8 (a) of Ref. [31]). This observation is the starting point of this study. What is the energy production error one may have if this modification of the downstream turbines behaviour is not taken into account? Mycek et al.'s experimental results are presented in Fig. 2 of Section 3 together with the present applied methodology.

In order to have a better knowledge of real ambient turbulence that a turbine may encounter in energetic sites, some researchers performed field measurements of turbulence in Fall of Warness, UK [35,36], Puget Sound, WA, USA [43,42], Sound of Islay, UK [27], Strangford Narrows, Ireland [21] and Paimpol-Bréhat, France [20,15]. These studies, all performed in possible future implementation sites, showed that the level of turbulence intensity may vary a lot, the lower limit being at 3.2% from the Strangford Narrows. Additionally, it has to be reminded that these levels of turbulence vary with tidal coefficients and also within a tidal cycle. The ambient turbulence aspect, together with many other aspects, really need to be accounted for when designing the implantation of tidal turbines within a farm. Several tools for turbines layout optimisation already exist in the literature [19,9,45,16]. Maslov et al. [25] also coupled that with a technico-economical approach. But do these numerical models accurately account for different levels of ambient turbulence? If so, do they properly model the modification of power coefficient for downstream turbines? If these aspects are not taken into account, will it largely modify the energy production and hence, the profitability of such turbine farms? The present paper will be an attempt to answer these questions.

In Section 2, the analytical model developed by Bahaj and Myers in 2004 is presented and validated in order to be used as a simple resource assessment for the purpose of the paper. Then, the modified semi-analytical approach developed here to account for ambient turbulence will be presented in Section 3. Three different scenarios of downstream turbine power coefficient modifications will be presented and the obtained results analysed. Finally, different yearly energy production cases of a idealised tidal turbines farm in the East-Race of Alderney will be presented and discussed. A technico-economical approach will also be carried out (Section 4) in order to assess the influence that these differences in the yearly energy productions may have on the profitability of such farms.

2. Bahaj and Myers' analytical model

The present paper aims at presenting an estimate of energy production losses due to ambient turbulence effects. In order to focus on the turbulence effects, the basic, robust and validated resource model developed by Bahaj and Myers [3] was a good option. A more complex model could have been used with more recent and more detailed flow characterisations but this was not the scope of the present study. This first section will basically reproduce, in a more synthetic way, the methodology developed by Bahaj and Myers in their 2004 study. The yearly energy production based on the data given for the East Race will be used as a validation of the procedure. The reader could refer to Ref. [3] for a more detailed description of the methodology.

Following the previous study [3], the chosen site was the Race of Alderney. This race lies on the West coast of France in the Channel sea between the island of Alderney and Cap de la Hague. This site is known as one of the most energetic in the world such as the Bay of Fundy in Canada or the Pentland First in the United Kingdom. The current velocity distribution for the West and East Races, during the spring and neap tides, can be seen in Fig. 1. From [3], an estimation of flow speed distribution between the spring and neap tides for the East Race were available and reproduced in Table 1.

The available power in a tidal current can be evaluated by the following equation:

$$P = \frac{1}{2}\rho A V^3, \tag{1}$$

where ρ is the sea water density, A is the rotor area and V is flow velocity. However, for many reasons (Betz limit, rotor design and blade profile, losses, etc.) only a fraction of this power can be retreived by any converter. So, the use of a power coefficient (C_P) is necessary in order to take into account for these factors inherent to the conversion of energy from mechanical to electrical. Eq. (1) then becomes:

$$P = \frac{1}{2}C_P\rho A V^3. \tag{2}$$

From the velocity variation depicted in Fig. 1 and the estimated hourly variation of Table 1, it is now possible to assess a daily estimate of energy production using Eq. (2). Now, from the velocities extrapolations between spring and neap tides given in Table 1, it is possible to assess a weekly estimate of energy production. Finally, as there is 52 weeks a year, a rough estimate of the yearly energy production can be obtained using the following equation:

$$\textit{Annual energy density}\ (\mathrm{kWh/m^2}) = \sum_{d=1}^{7}\sum_{h=1}^{13}\left[\frac{1}{2}\rho V_{h,d}^3\right] \times \frac{24}{26} \times 2 \times 52, \tag{3}$$

where the correction coefficient of 24/26 had to be introduced for a 24-h energy production similarly to the work of Bahaj and Myers [3]. Additionally, it is assumed that the two tidal cycles a day have the same velocity records.

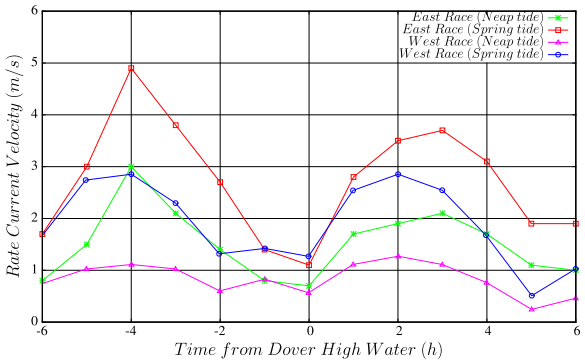

Fig. 1. Variation of marine current velocity in the Alderney Race relative to Dover High Water (data reproduced from Fig. 2 and Table 1 of Bahaj and Myers [3]).

Table 1
Flow speed distribution between spring and neap tides for the East Race of Alderney (data reproduced from Table 1 of Bahaj and Myers study [3]).

Dover high water (h)	Current speed at intervals (m/s)						
	Spring tide	+1 day	+2	+3	+4	+5	Neap tide
−6	1.7	1.6	1.4	1.3	1.2	1.0	0.8
−5	3.0	2.8	2.6	2.3	2.1	1.9	1.5
−4	4.9	4.7	4.4	4.1	3.8	3.5	3.0
−3	3.8	3.6	3.3	3.1	2.9	2.6	2.1
−2	2.7	2.5	2.3	2.1	2.0	1.8	1.4
−1	1.4	1.3	1.3	1.2	1.1	1.0	0.8
0	1.1	1.1	1.0	0.9	0.9	0.8	0.7
1	2.8	2.6	2.5	2.3	2.2	2.0	1.7
2	3.5	3.2	3.0	2.8	2.6	2.4	1.9
3	3.7	3.5	3.3	3.0	2.8	2.6	2.1
4	3.1	2.9	2.7	2.5	2.3	2.1	1.7
5	1.9	1.8	1.7	1.5	1.4	1.3	1.1
6	1.9	1.8	1.6	1.5	1.4	1.2	1.0

Table 2
Final yearly energy production obtained by Bahaj and Myers and reproduced from Ref. [3] compared with the present results. The use of the sign – for the present study means that exactly the same value was chosen as in Ref. [3]. The error in the energy production is 2.54% for the East race and 12.36% for the West race.

Nominal depth (m)	Rotor diameter (m)	West Race				East Race			
		Rating of 16 twin rotor sub-array (MW)	Number of sub-arrays	Swept area (m^2)	Present study	Rating of 16 twin rotor sub-array (MW)	Number of sub-arrays	Swept area (m^2)	Present study
28	14	12	9	44334	–	49	34	167485	–
36	20	24	14	140743	–	99	4	40212	–
40	25	38	16	251327	–	155	1	15707	–
Total swept area (m^2)				436,404	–			223,404	–
Energy density (kW h/m^2)				20,954	18,331			72,448	74,186
Annual energy (TW h)				2.67	2.34			4.73	4.85

Previous Eq. (3) can now be considered as to simplistic as more accurate models now exist [33,25]. In this annual energy density equation, no variation of tidal coefficient is considered. Additionally, the correction coefficient to fit to a 24-h day may seems too simplistic. For the Alderney Race, hourly velocity records are now available for many years from numerical computations performed by IFREMER, the Previmer data base [38] for instance. However, as already mentioned, the aim of the present study is to focus on the turbulence effect on the energy production. The use of the Bahaj and Myers 2004 [3] analytical model was motivated by its simplicity so that emphasise could be made on the turbulence effects.

In order to validate the present methodology, the annual energy production presented in [3] for the East race zone was recomputed using the same turbine numbers and sizes. This East race zone was chosen here because more detailed velocity variations were given in Table 1 of Ref. [3], which were not available for the West race. It is necessary to mention that where current velocities were less than 1.1 m/s (minimum operating flow speed), the energy potential of the tidal stream was ignored. Once determined the energy density corresponding to the East Race of Alderney using Eq. (3), the annual energy output was obtained as follows:

$$\textit{Annual energy output}\ (\mathrm{kWh}) = \textit{Annual energy density}\ (kWh/m^2) \times\ \textit{Swept area}\ (m^2)\ \times\ C_P. \tag{4}$$

Regarding the turbine numbers and sizes, twin rotor machines were considered installed in sub arrays of 16 units, separated by a distance of 18 diameters between the two rows of 8. The spacing between sub-arrays was at least 500 m. Three different rotor sizes were adopted, with diameters of 14, 20 and 25 m. The number of sub-arrays chosen for each rotor diameter, for the West and East Race, can be seen in Table 2. Finally, the swept area for each type of turbine and the total one was calculated and also reproduced in Table 2. The power coefficient was assumed as 0.30 for all calculations. For the downstream row in each sub-array, the power generated was supposed to be 0.95 that of the upstream machines, to take into account the velocity reduction due to the wake effect. In Ref. [3], no velocity deficits were considered between sub-arrays, since the space between them is supposed to be large enough. In the following sections, these two aspects, namely the power coefficient correction and velocity deficits, will be highlighted and discussed.

Following the methodology described above and using the same current velocity values, the energy density and annual production was calculated for the Race of Alderney. All the obtained results are shown in Table 2 and compared with those of Bahaj and Myers. The 2.54% error for the East race probably corresponds to a round off error in the variation of Table 1 reproduced from [3], where only one digit values were given. In fact, the evaluation of Bahaj and Myers may have been performed with 2 or 3-digit numbers. For the case of the West Race, there was no other choice than extracting the data from Fig. 2 of Ref. [3] and then assume a linear variation between the spring and neap tides in order to obtain the values for the other days of the week as in Table 1. This possibly explain why a higher error is observed for the West Race with 12.36%. However, the energy production for the East race is very accurate with respect to the given data and the present reproduced methodology can now be considered as validated. The following section will now present how the experimental results of Mycek et al. [31] regarding the turbulence influence can be incorporated in the analytical model.

3. Semi-analytical model to account for ambient turbulence

Ambient turbulence intensity I_∞ is defined as:

$$I_\infty = 100\sqrt{\frac{\frac{1}{3}\left[\sigma^2(u_\infty)+\sigma^2(v_\infty)+\sigma^2(w_\infty)\right]}{\overline{u}_\infty^2+\overline{v}_\infty^2+\overline{w}_\infty^2}}, \tag{5}$$

where the velocity components $u_\infty, v_\infty, w_\infty$ are those of the upstream velocity $\mathbf{u}_\infty$, $\overline{\mathbf{u}}_\infty$ is the time average of $\mathbf{u}_\infty$ and $\sigma(\cdot)$ represents the standard deviation of the value $\cdot$. The ambient turbulence intensity of a site, where turbines are installed, plays a major role in the energy production of the turbine farm. Its influence is all the more important as the turbines aligned with the main flow direction are close together. In fact, the wake of an upstream turbine will deeply affect the performance of the

turbine positioned downstream. And ambient turbulence not only influences the wake development but also the downstream turbines performance itself. In the following, experimental datasets from the work of Mycek et al. [31] will be post-treated in order to feed with fitted equations the developed semi-analytical model. Then, a special care will be made for the treatment of the downstream turbines C_P. Finally, for an ideal set-up of turbines aligned with the flow, differences in the energy production will be evaluated depending on how this C_P coefficient is estimated.

3.1. Fitted equation obtained from experimental data

From the first part of the work of Mycek et al. [30], power coefficient curves were evaluated for different ambient turbulence intensities and, for a given I_∞ with different upstream velocities. Fig. 6 (a) of Ref. [30] (page 736) shows that these C_P-curves are very similar for different incoming velocities for $I_\infty = 3\%$. To a smaller extent for $I_\infty = 15\%$, Fig. 6 (b) from the same Ref. [30] (page 736) also depicts that these C_P-curves reveal to be similar for different incoming velocities. However, the average C_P-curve for $I_\infty = 3\%$ is slightly different from the one for $I_\infty = 15\%$. These experimental observations were further confirmed in a round robin test [17] with the same turbine installed in different flume tanks or towing tanks. In the operating range, the grey zone in both Figures, the C_P is rather constant and an average could be performed for each ambient turbulence. In the case of 3%, a value of $C_{P_{3\%}} = 0.41$ was obtained, the curve corresponding to an incoming velocity of 0.4 m/s being discarded for the reasons explained in the experimental paper [30]. For 15%, a slightly lower value of $C_{P_{15\%}} = 0.35$ was calculated. This leads to the conclusion that, for this given turbine, the maximum power coefficient depends on the ambient turbulence intensity. But, for a given ambient turbulence intensity, this maximum power coefficient is somehow constant for a reasonable range of Tip Speed Ratio (*TSR*) and incoming velocity.

In the second part of the work of Mycek et al. [31], the authors defined a downstream turbine efficiency (η) depending on the perceived velocity and the ambient turbulence I_∞. η was evaluated for different positions in the wake of an upstream turbine. Eq. (6) presents a synthetic form of Eq. (11) presented in the experimental paper [31]:

$$\eta_{I_\infty}(x) = \frac{C_{P,I_\infty}(V(x))}{C_{P,I_\infty}(U_\infty)}, \tag{6}$$

with the power coefficient C_P defined using Eq. (2) either using the really perceived disk-integrated velocity $V(x)$ or the infinite upstream velocity U_∞. The perceived disk-integrated velocity $V(x)$ is well defined in Section 2.8 of Ref. [30]. Fig. 2 depicts the efficiency of the downstream turbine η as a function of the inter-device distance a/D, where a is the separation between devices and D the rotor diameter, for two different values of turbulence intensities ($I_\infty = 3\%$ and 15%). From this Fig. 2, it can be observed that $\eta_{I_\infty=15\%}$ is always assumed to be 100% [1] and that $\eta_{I_\infty=3\%}$ varies a lot starting from $\approx 60\%$ and then increasing. This does not mean that a turbine immersed in a flow at $I_\infty = 15\%$ 5 or 10 diameters downstream of an upstream one will produce the same power. It only means that their C_P, evaluated with Eq. (6) using either U_∞ for the upstream turbine or $V(x)$ for the downstream one, will be the same. This is basically the assumption made numerically when using a porous disk approach. In fact, in such numerical approach, the power of a given turbine depends on the perceived velocity $V(x)$ but the C_P-value is constant. The experimental results used in this paper prove that this assumption is true for a high level of ambient turbulence, here $I_\infty = 15\%$. However, this assumption that the C_P coefficient is a constant is no more valid for downstream turbines immersed in a lower ambient turbulence. This is clearly observable in the 3% ambient turbulence case as depicted in Fig. 2.

The following of the present paper will be dedicated to an evaluation of the error made if one assume that the C_P coefficient is constant in the wake of an upstream turbine. For the following semi-analytical numerical analysis, the efficiency η corresponding to the ambient turbulence of 15% was assumed as $\eta_{I_\infty=15\%} = 100\%$ for all the inter-device distances. In the case of $I_\infty = 3\%$, an approximated equation was fitted from the experimental points (see Fig. 2) first in order to have approximated values of $\eta_{I_\infty=3\%}$ for all the x-values in the studied range but also in order to cover a higher range of distances between turbines up to $a/D = 25$. The fitted equation is a combination of an exponential function for the portion where experimental information was available and a linear assumption for the rest:

$$\eta_{I_\infty=3\%} = \begin{cases} \frac{-25.076}{1+e^{x^*-5.8}} + 85 & x^* < 9 \\ 0.944x^* + 75.522 & x^* \geqslant 9 \end{cases}, \tag{7}$$

where x^* denotes x/D. Fig. 2 depicts the experimental curves together with their fitted equation for $\eta_{I_\infty=3\%}$ (Eq. (7)) and $\eta_{I_\infty=15\%} = 100\%$. The linear approximation for $x^* \geqslant 9$ could be questionable but, to the authors' knowledge, no experimental values are available. And the slope of this linear approximation is calculated to have a continuity from the range of a/D where experimental values exist ($x^* \leqslant 10$) and where extrapolation is assumed.

Now that semi-analytical equations are obtained for the C_P-coefficient, the same procedure needs to be performed for the evaluation of velocity in the wake. In the experimental study [31], disk-integrated velocity deficits ($\gamma(x^*) = V(x^*)/U_{up}$) are also presented depending on the ambient turbulence. Both graphs of Fig. 3 reproduce these experimental velocity deficits. The evaluation was performed in the wake of a single turbine: in that case the equation of the velocity deficit was

[1] If the experimental values are slightly above 100%, it is mainly due to small experimental errors that are emphasised by the power of 3 in Eq. (2) and the integration process. This artefact is largely discussed and detailed in Mycek et al.'s paper [31].

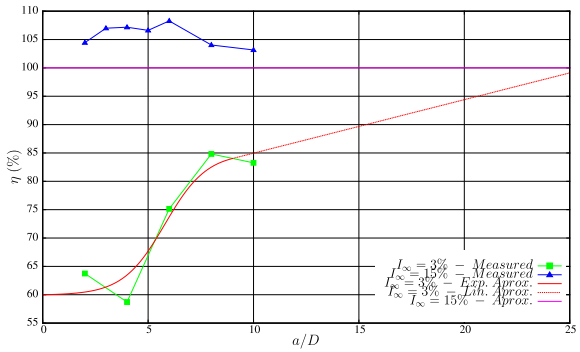

Fig. 2. Efficiency of the downstream turbine function of the dimensionless inter-device distance a/D depending on the ambient turbulence intensity I_∞. Data are reproduced from Ref. [31].

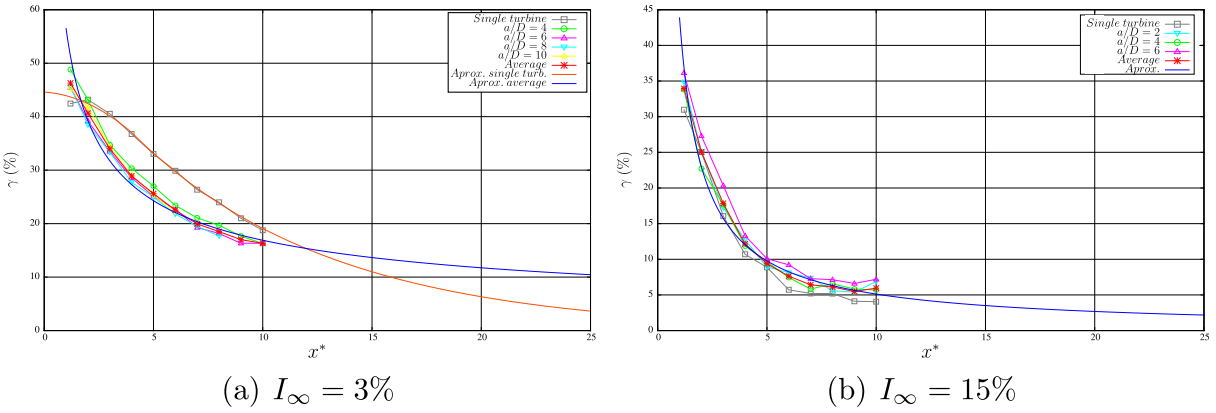

Fig. 3. Velocity deficit in the wake of the downstream turbine for various distances between the devices (data from Ref. [31]).

$\gamma(x^*) = V(x^*)/U_\infty$; or in the wake of the second turbine, the definition of the velocity deficit becoming then $\gamma(x^*) = V(x^*)/V_{up}$, where V_{up} is the velocity that is measured just in front of this second turbine. All these curves are reproduced from Ref. [31] and similarly, fitted equations are calculated. For the situation of $I_\infty = 3\%$ of ambient turbulence, a distinction was made between the wake of a single turbine and the others. In fact, the wakes behind the second turbine are very similar whatever the inter-device distance between the first and the second turbine is (see Fig. 3 (a)). This is very convenient as a single fitted equation (Eq. (8)) can be estimated for these latter cases from an average of all the experimental curves:

$$\gamma_{I_\infty=3\%} = 56.467x^{*-0.524}. \tag{8}$$

For the wake behind a single turbine (or the first turbine), the fitted Eq. (9) is obtained:

$$\gamma_{I_\infty=3\%(Single\ \ turbine)} = \begin{cases} -0.402x^{*2} - 0.282x^* + 44.605 & x^* < 4 \\ 57.612e^{-0.1104x^*} & x^* \geqslant 4 \end{cases}. \tag{9}$$

With respect to the case of $I_\infty = 15\%$, all the curves representing the disk-integrated velocity deficits superimpose (see Fig. 3 (b)), although this tendency is less clear than previously. The obtained velocity deficit equation was also constructed from an average of the experimental curves as:

$$\gamma_{I_\infty=15\%} = 43.855x^{*-0.933}. \tag{10}$$

Now that the experimentally fitted equations are obtained, the developed methodology can be presented.

3.2. Methodology, results and analysis

In order to evaluate the influence that turbulence intensity have on the energy production of a turbines farm, a simple case of analysis was carried out. In fact, in the present model, only the interactions between turbines aligned with the flow

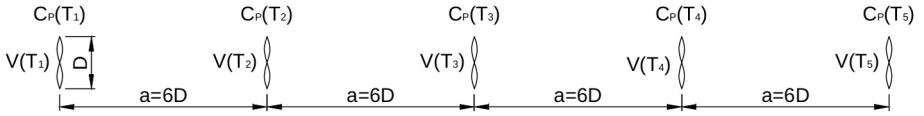

Fig. 4. Scheme of the considered idealised farm configuration with 5 turbines aligned with the flow direction.

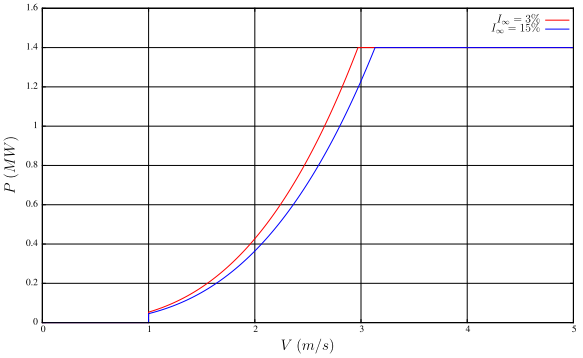

Fig. 5. Power curves.

are considered. Neither lateral interactions nor venturi effect can be considered. In that case, the idealised farm configuration basically reduce to N turbines aligned with the flow direction as depicted on Fig. 4, with $N = 5$.

The turbine model is a 3-bladed turbine of 18 meters diameter. The cut-in velocity is supposed to be 1 m/s and a rated power of $1,4$ MW was selected. Fig. 5 depicts the power curves of this idealised turbine for $I_\infty = 3\%$ and $I_\infty = 15\%$. The slight difference between the two curves lies in the fact that $C_{P_{3\%}} = 0.41$ and that $C_{P_{15\%}} = 0.35$ as mentioned above. Still, both curves of Fig. 5 are similar and exhibit nearly the same rated velocity of ≈ 3 m/s. The parameter of the considered turbine model are very close to those of the Alstom's Oceade turbine, although the exact C_P values are unknown to the authors for evident confidentiality reasons. This choice was motivated in order to be closer to reality as such turbines will really be deployed in the Alderney Race. And such interaction between aligned turbines will really exist as one can see on the implantation scheme of the Nepthyd project presented in Fig. 3 of Ref. [13]. In fact turbines denoted $A3$ and $A18$ will experience such interaction as they are aligned with the main flow and settled at nearly the same depth: 38 m for the first and 39 m for the the second. The density of salted water is supposed here to be approximately 1023 kg/m^3.

In order to explain the methodology, a first case of analysis was developed based on the schematic representation of Fig. 4. It consists of 5 turbines separated by an inter-device distance of 6 diameters. For this given example, the incoming flow velocity is fixed to $U_\infty = 4$ m/s. Each turbine will be named T_n, n being its position in the column: for instance, the first turbine is T_1, the second is T_2 and so forth. Two important pieces of information need to be determined for each turbine: first, the perceived velocity $V(T_n)$ just in front of the turbine and seconds, its power coefficient based on this perceived disk-integrated velocity $C_P(T_n)$. Of course, this two values will depend on the considered ambient turbulence intensity I_∞.

For the first turbine, the perceived velocity is $V(T_1) = U_\infty$ and γ_1 basically reduces to zero. For the velocity perceived by the second turbine, $V(T_2)$ is obtained with the value of $\gamma_2(x^* = 6) = 29.71$ from Eq. (9) for $I_\infty = 3\%$ (Fig. 3 (a)) or $\gamma_2(x^* = 6) = 0.825$ from Eq. (10) for $I_\infty = 15\%$ (Fig. 3 (b)). For the third turbine and the followings, the procedure is reproduced, the only difference being that the value of $\gamma_3(x^* = 6) = 22.07$ is obtained from Eq. (8) for $I_\infty = 3\%$. Eq. (11) present a summary of the velocity methodology for each turbine:

$$\begin{aligned} V(T_1) &= U_\infty(1 - \gamma_1/100) = U_\infty \\ V(T_2) &= U_\infty(1 - \gamma_1/100)(1 - \gamma_2/100) \\ V(T_3) &= U_\infty(1 - \gamma_1/100)(1 - \gamma_2/100)(1 - \gamma_3/100) \\ V(T_4) &= U_\infty(1 - \gamma_1/100)(1 - \gamma_2/100)\ \ldots\ (1 - \gamma_4/100) \\ V(T_5) &= U_\infty(1 - \gamma_1/100)(1 - \gamma_2/100)\ \ldots\ (1 - \gamma_5/100) \end{aligned} \tag{11}$$

All these results are summarised in Table 3 and depicted on Fig. 6(a). Using an adequate CFD solver would probably have given similar results. Even if this seems to be very simple from these analytical equations based on experimental results, obtaining such result numerically is not trivial. One has to properly reproduce the effect ambient turbulence have on the wakes. This is absolutely not as straightforward.

However, the main focus of this paper is to assess the error one would make using an erroneous formulation of the power coefficient C_P. In fact, as mentioned earlier, some numerical approaches use a constant value for C_P. From the experimental

Table 3
Results for the case of analysis.

Turb.	a/D	γ (%)		V (m/s)		C_P				P (MW)			
		3%	15%	3%	15%	3% pes.	3% opt.	3% cst.	15%	3% pes.	3% opt.	3% cst.	15%
T_1	0	0	0	4	4	0.41	0.41	0.41	0.35	1.40	1.40	1.40	1.40
T_2	6	29.71	8.25	2.81	3.67	0.30	0.30	0.41	0.35	0.87	0.87	1.19	1.40
T_3	6	22.07	8.25	2.19	3.37	0.30	0.35	0.41	0.35	0.41	0.48	0.56	1.40
T_4	6	22.07	8.25	1.71	3.09	0.30	0.35	0.41	0.35	0.20	0.23	0.27	1.34
T_5	6	22.07	8.25	1.33	2.84	0.30	0.35	0.41	0.35	0.09	0.11	0.13	1.04
										2.98	3.09	3.54	6.58

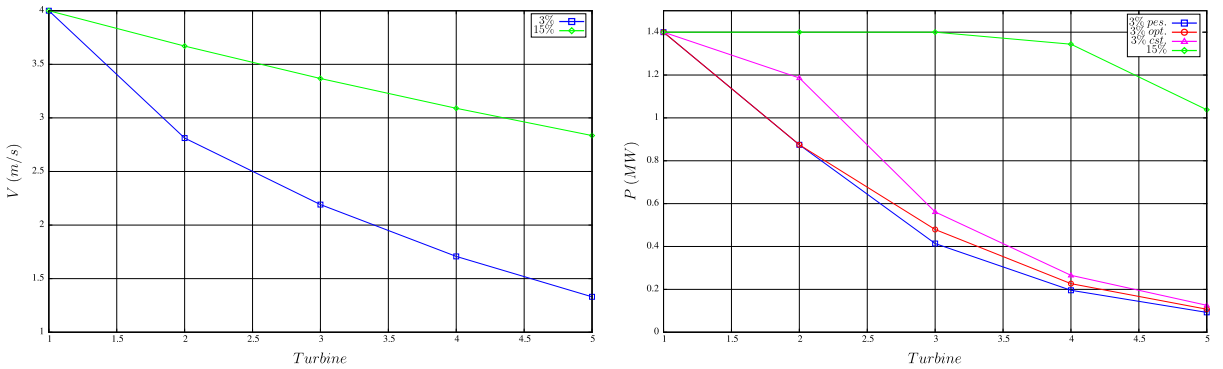

(a) Velocity perceived by each turbine. (b) Power generated by each turbine.

Fig. 6. Curves for the case of analysis.

observations of Mycek et al. [30], Gaurier et al. [17] and others, this assumption is wrong as the maximum C_P-value sightly differ from 0.41 for $I_\infty = 3\%$ to 0.35 for $I_\infty = 15\%$. In most recent numerical studies focusing on turbulence influence, these variations were taken into account and the C_P-values were depending on the turbulence intensity. But still, this C_P-value was a constant for all turbines (upstream and downstream) once this ambient turbulence was decided. This last assumption is true for high values of turbulence intensities as experimentally observed by Mycek et al.'s Part II [31] and presented on Fig. 2 for $I_\infty = 15\%$. Although this affirmation is only based on the experimental values obtained for a given turbine and the higher ambient turbulence. With another turbine geometry, the affirmation may not be true any more. And, in any case, the minimum value of ambient turbulence for which this affirmation is true is not clearly defined in the literature.

For this semi-analytical approach, the value of C_P will set to a constant value of $C_P = 0.35$ for $I_\infty = 15\%$. However, three scenarios will be considered for the lower turbulence intensity of $I_\infty = 3\%$:

- a *constant approach*, where a value of $C_P = 0.41$ is set for all turbines and which is obviously not the case experimentally,
- a *pessimistic approach*, where a value of $C_P = 0.41$ for the first turbine and 0.30 for the following ones. This last value is obtained from Eq. (7) for $x^* = 6$,
- a *optimistic approach*, where a value of $C_P = 0.41$ for the first turbine, $C_P = 0.30$ for the second and $C_P = 0.35$ for the following ones. This *optimistic approach* is based on the fact that in the wake of a second turbine, turbulence is much increased (see Fig. 9 (c) of Ref. [31]) and the third turbine would act as if it was immersed in a 15% ambient turbulence flow.

Both *pessimistic approach* and *optimistic approach* are based on hypothesis that need to be further validated. However, these approaches are probably more accurate than the *constant approach* which is obviously erroneous at this lower ambient turbulence intensity. The *pessimistic approach* and *optimistic approach* probably represent an envelop of what would really happen in reality. The only way of assessing this assumption would be to carry out large experimental trials with, at least, three or more aligned turbines. Numerically, only a full Navier Stokes approach would be able to give reliable results. However, to the authors knowledge, this was not performed up to now for such a configuration. And other porous-disk + CFD, blade element momentum theory + CFD, actuator line + CFD, even boundary element methods will encounter difficulties in modelling the C_P modification accurately.

Fig. 6 depicts the obtained results in terms of velocity (Fig. 6(a)) and in term of generated power (Fig. 6(b)) for each of the 5 turbines considered in the schematic representation of Fig. 4. Both graphs reproduce the data detailed in Table 3. As scheduled, it is striking to observe how different would behave the same farm if immersed in a $I_\infty = 3\%$ ambient turbulence

intensity flow or in a $I_\infty = 15\%$ one. In the case of higher turbulence, the 3 first turbines operate at rated power and the fourth and fifth with only a reasonable loss. Whereas for the case of $I_\infty = 3\%$, the power generated by the second turbine is already largely altered and the fith turbine hardly produce 0.1 MW from its 1.4 MW nominal power. In terms of cumulative power, a overall 6.58 MW is obtained for the $I_\infty = 15\%$ case whereas less than 50% of this value is obtained for $I_\infty = 3\%$ whatever the scenario is.

Regarding the difference between the different scenarios in the case of low ambient turbulence ($I_\infty = 3\%$). First, from Fig. 6(b), it can be observed that the *pessimistic approach* or *optimistic approach* more or less give the same results. As a consequence, cumulative power is nearly similar with 2.98 MW for the *pessimistic approach* and 3.09 MWor the *optimistic* one. This results in less than 3.7% error in terms of comparison. This estimated error may be acceptable in terms of engineering but, for the long term energy production, this may affect the project profitability. This is going to be assessed in the following Section 4.

However, to the authors knowledge, most of the resource assessment and energy production studies for future commercial farms are performed with a *constant approach* for the C_P, taking into account for I_∞ but constant for all turbines in a given computation. And, in the case of low I_∞, it is critical as more than 12.7% of over-estimation is computed with such an assumption (3.54 MW instead of the $\approx$ 3.0 MW for the two other approaches). Again, for the long term energy production and profitability, this will affect the project viability. The present study is based on experimental data extrapolated at real scale, for a given turbine geometry and some other hypothesis were assumed in order to obtain fitted equations. Additionally, such a low ambient turbulence intensity of $I_\infty = 3\%$ may not be found in many energetic sites. But some site as the Strangford narrow, where the first 1.2 MW Seagen turbine was installed encountered such low ambient turbulence. For more detail, the reader can refer to Table 1 of Ref. [30], where interpretation of Mac Enri et al.'s values [21] was detailed.

To conclude, the main question that remains from this analysis is: what is the lower I_∞-limit at which the C_P-values do not change as in the case of $I_\infty = 15\%$? This clearly is an unknown and further studies on this topic would be of great scientific interest. Therefore additional studies on the effect of ambient turbulence in the framework of tidal turbine in a farm may prove to be of prior importance in the near future.

4. Technico-economical application to a possible farm in the Alderney Race

In this section, a concrete example of application will be carried out. As the present model does not take into account for lateral interaction, the behaviour of a single column of turbines oriented in the current direction is studied in order to evaluate the influence that ambient turbulence has on the total energy production, as a function of the inter-device distance. Finally, an economic analysis is developed based on a 20 years period of energy production.

In order to follow an engineering approach, the dimensions allowed for the installation of the farm will be given and the number of turbines to be installed will be the output. A total length of 400 meters is considered here. This is somehow in accordance with the recent concessions made by the French government to the NEPTHYD project ($\approx$ 430 m $\times$ $\approx$ 550 m in width and length respectively, see Fig. 3 of Ref [13]) and the Normandy Hydro project ($\approx$ 570 m $\times$ $\approx$ 480 m in width and length respectively, see Fig. 3 of Ref [14]). The length is defined here as the dimension aligned with the main flow direction. So far the number of turbines is concerned, 14 set-ups were tested with between 2 and 15 devices equally spaced. Given the 400 meters allowed here and the 18 meters for the turbine diameter, a inter-device distance range between $1.59D$ (for 15 turbines) and $22.22D$ (for twin turbines configuration) is considered. For the turbulence intensity, similarly, the two values of 3% and 15% are adopted. For the case with 3% of ambient turbulence, the same three scenarios as in previous Section 3.2 were analysed, namely the *pessimistic*, the *optimistic* and the *constant approach* with respect to the account of C_P.

In order to evaluate the energy production, the methodology developed in Section 2 for the tidal resource is adopted. As already discussed in this above mentioned section, a more recent and more accurate model could have been adopted. But the main focus of the present paper is more assessing the error one may have, when using a constant C_P-value, in evaluating the tidal farm energy production than the actual amount of energy produced.

More particularly, the energy production was computed from the tidal cycles of the East Race, from spring to neap tide as depicted in Table 1. For each infinite upstream velocity (depending of the day and time in the tidal cycle) and for each inter-device distance, the aforementioned analysis of Section 3.2 is carried out. To be more precise, for every hour (corresponding to a given velocity in Table 1), the perceived velocity $V(T_n)$ (Eq. (11)), the power coefficient value $C_P(T_n)$ (Eq. (6)) and finally the energy production of each turbine is computed as in Table 3. Then, for each turbine, the yearly energy production is evaluated from Eq. (3) adapted in order to account for the considered C_P-scenario and the swept area of the turbine (A):

$$Energy\ (kWh) = \sum_{d=1}^{7}\sum_{h=1}^{13}\left[\frac{1}{2}\rho V_{h,d}^3 C_P(T_n)\right] \times \frac{24}{26} \times 2 \times 52 \times A. \tag{12}$$

For the economical assessment, it is really complicated to obtain comprehensive information regarding the cost of turbines. In that respect, the cost of a tidal turbine was calculated from Maslov et al. [25], where a 0.5 MW marine current turbine was estimated at 4.76 millions of euros (including foundation, manufacturing, installation on site, dismantling, maintenance, electric system, etc.). So that, for the considered 1.4 MW tidal turbine, this cost will be extrapolated to

Table 4
Number of turbines, dimensionless inter-device distance a/D, yearly energy production in GWh and net incoming in $M€$ on a 20 years basis. Comparison between the 3% and 15% of ambient turbulence. For the 3% ambient turbulence case, the three scenarios of Section 3.2 are analysed regarding the C_P evaluation.

No. turb.	a/D	Yearly energy production (GWh)				20 years based net incoming ($M€$)			
		3% pes.	3% opt.	3% cst.	15%	3% pes.	3% opt.	3% cst.	15%
2	22.22	10.56	10.56	10.67	9.93	21.75	21.75	22.27	18.85
3	11.11	11.28	11.27	11.96	13.95	11.71	11.65	14.85	23.93
4	7.41	10.07	10.18	11.01	16.58	−7.15	−6.64	−2.86	22.66
5	5.56	8.61	8.86	9.69	17.60	−27.14	−26.02	−22.21	14.04
6	4.44	7.72	7.94	8.72	17.24	−44.57	−43.56	−39.99	−0.94
7	3.70	7.24	7.41	8.15	16.03	−60.07	−59.29	−55.92	−19.84
8	3.17	6.97	7.11	7.84	14.50	−74.62	−73.99	−70.65	−40.16
9	2.78	6.83	6.94	7.62	13.07	−88.60	−88.10	−84.96	−60.01
10	2.47	6.72	6.81	7.45	11.90	−102.43	−102.03	−99.07	−78.71
11	2.22	6.66	6.73	7.35	10.97	−116.04	−115.70	−112.84	−96.27
12	2.02	6.60	6.66	7.27	10.19	−129.61	−129.34	−126.56	−113.18
13	1.85	6.56	6.61	7.20	9.53	−143.13	−142.90	−140.19	−129.53
14	1.71	6.52	6.56	7.14	9.02	−156.61	−156.43	−153.78	−145.19
15	1.59	6.50	6.53	7.10	8.54	−170.04	−169.89	−167.28	−160.69

13.32 millions of euros. This cost is somehow in coherence with the price range given by Prof. A.S. Bahaj in his review paper of 2011 [2]. The feed in tariff is evaluated to 229€ per MWh, still based on data from Maslov et al. [25]. For the operational maintenance, Maslov et al. decided to incorporate it in the total cost estimation as presented in the Table 8 of Ref. [25].

Table 4 presents the yearly energy production in *GWh* and the net incomings in $M€$ on a 20 years basis depending on, the number of turbines (and hence the inter-device distance) and the ambient turbulence intensity. Fig. 7 graphically reproduces the results presented in Table 4 for the energy production. From these results, it can be observed that the maximum yearly energy production for $I_\infty = 15\%$ with ≈ 17.6 GWh is much more than the ≈ 11.9 GWh for the lower ambient turbulence at $I_\infty = 3\%$. The yearly energy production for $I_\infty = 15\%$ approximately represents an increase of 48% with respect to the $I_\infty = 3\%$-case. As a matter of partial conclusion, two conclusions can be drawn: the account of ambient turbulence is absolutely not negligible in the producible assessment of a given site and higher ambient turbulence sites should be preferred in terms of energy production. However, such environment is more stressful for the device. In fact, experiments [31] showed that the standard deviations of power C_P and thrust C_T coefficients are increased with higher ambient turbulence, leading to more fatigue to the turbine and supporting structure.

Another observation from Fig. 7 is that, as scheduled, the turbine layout may largely depend on the ambient turbulence. In fact, for the higher ambient turbulence, the most suitable number of turbines to distribute along the column is 5, leading to an inter-device distance of 5.56 diameters. On the contrary, for the lower I_∞ value, it is better to install only 3 turbines, separated with a distance of 11.11 diameters. This observation was nearly straightforward from the wake maps analysis presented in Ref. [31]. However, such a difference on the total energy production was not easily predictable and reveals to be surprisingly high. This unexpectedly large different can be explained by some thresholds effects with respect to the turbine cut-in velocity for the lower velocities in the tidal cycle. Coming back to the turbine layout, the optimal set-up of turbines may be complicated to identify as ambient turbulence intensity vary within a tidal cycle as several researchers observed in different potential sites. In that respect, the study of Mac Enri et al. [21], Thompson et al. [42], Filipot et al. [15] are relevant. For instance, a variation from $I_\infty = 3.2\%$ to 7.1% was observed in the Strangford Narrows by Mac Enri et al. [21].

Finally, regarding the different scenarios for the $I_\infty = 3\%$-case, a nearly constant over-estimation of the yearly energy production between ≈ 0.6 and ≈ 0.8 GWh is found with the *constant approach* for the C_P model. To the authors belief, this excess of ≈ 0.6 to ≈ 0.8 GWh is erroneous and may lead to an over-estimation of the turbine farm incomings at the study phase. Will this overestimation of nearly 6.1%, for the optimal 3 turbines configuration, be significant in the following economical assessment? Fig. 8 will present some first pieces of analysis on that topic.

In terms of incoming after 20 years of production, Fig. 8 graphically depicts the values presented in Table 4. The results approximately follows the same conclusions presented above although that some tendencies are sharper. For instance, for the $I_\infty = 15\%$ ambient turbulence case, the optimal set-up of 5 turbines in terms of total energy production is no more the economic optimum with a positive result of only 14 $M€$ approximatively. In fact, both 3 and 4 turbines configurations with respectively 24 $M€$ and 22.7 $M€$ maximise the net incomings. However, the 6 turbines configuration directly drops to a negative result with approximatively -1 $M€$. And then, worse and worse results are obtained by adding new turbines.

For the lower ambient turbulence case ($I_\infty = 3\%$), the most profitable option will be to install only 2 turbines with approximately 22 $M€$ whatever of the C_P scenario is. In fact, with only 2 turbines, the *pessimistic* and *optimistic approach* rigorously give the same results as presented in Table 4. And for such an inter-distance of ≈ 22 diameters, the turbine efficiency nearly recovered to a 100%, as depicted in Fig. 2. In the case of 3 turbines configuration, the *pessimistic* and *optimistic approach* also nearly give the same results with ≈ 11.7 $M€$. No real difference between these two scenarios can be observed at this stage. And increasing the number of turbine will slightly increase the difference but always with a

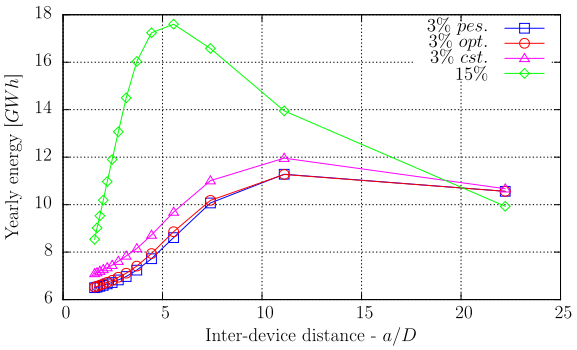

Fig. 7. Evolution of the yearly energy production in *GWh* with the number of installed turbines and presented with respect to inter-device distances. Comparison between the 3% and 15% of ambient turbulence. For the 3% ambient turbulence case, the three scenarios of Section 3.2 are analysed regarding the C_P evaluation.

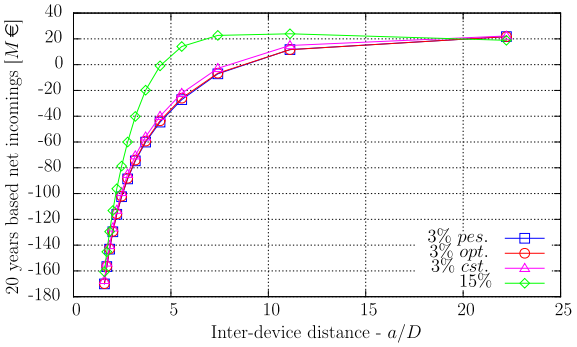

Fig. 8. Evolution of 20 years based net incomings in *M€* with the number of installed turbines and presented with respect to inter-device distances. Comparison between the 3% and 15% of ambient turbulence. For the 3% ambient turbulence case, the three scenarios of Section 3.2 are analysed regarding the C_P evaluation.

negative profitability, which makes such a difference in the C_P model useless in terms of practical interest. However, the *constant approach* overestimates the profitability by nearly 26.5% with $\approx$ 14.8 *M€* instead of $\approx$ 11.7 *M€* more realistically in this 3 turbines configuration. Such a difference of more than 25% in the farm profitability is worth investigating in order to obtain further validation.

5. Conclusions

The purpose of the present paper was to study the influence that ambient turbulence has on the energy generation of an idealised tidal turbine farm. The analytical model of Bahaj and Myers [3] is used in order to assess the tidal resource and hence, the energy production. This analytical model is modified to account for the influence of two different ambient turbulence levels. Experimental results of Mycek et al. [31] serve as input data in this modification procedure. The developed semi-analytical model is first validated against previous results in the literature.

The account of ambient turbulence influence is not only in the wake evaluation, which is commonly studied by the scientific community. But the power coefficient (C_P) modifications of the downstream turbine(s) are also considered, which is rather new. In that respect, for the lower ambient turbulence case, three different scenarios are considered which are: the *constant approach* frequently used in the literature, the *pessimistic* and *optimistic approach*.

For the given parameters of this study, the negligence of ambient turbulence on the considered idealised 5 turbines configuration showed an over-estimation of $\approx$ 50% in the power production. A more detailed model taking into account for the ambient turbulence but with the *constant approach* still exhibits a 12.7% overestimation on the same configuration if compared to the *pessimistic* or *optimistic approach*.

These last two scenarios come from analyses and extrapolations of experimental datasets. The related assumptions need to be further validated but, to the authors belief, they already are more accurate than the usually adopted *constant approach*. The main question that remains after the present study is: what is the lower I_∞-limit at which the C_P-values do not change as in the case of $I_\infty = 15\%$? And, another related question would be: will this behaviour be similar for other turbine geometry? These questions are not answered yet. And numerous experimental trials or massive numerical computations will be required to answer these questions.

To further analyse the differences owing to the ambient turbulence levels and the C_P model used for the lower ambient turbulence case, a concrete example of turbine layout study is performed for a given 400 m long site in the Alderney Race. An hypothetical configuration of several turbines aligned with the flow direction is studied, as no lateral interactions are accounted in the present model. The aims were first, to maximise the energy production for this given concession by varying the number of installed turbines depending on the ambient turbulence levels and, second, to evaluate an economical optimum. In terms of maximising the energy production, the number of turbines to be installed is very different depending on the ambient turbulence level. Unsurprisingly, 5 turbines had to be considered with the higher 15% ambient turbulence level and only 3 with the lower 3% case, for the given turbine definition, concession size and tidal resource. But, as a matter of result, an increase of approximately 48% in the yearly energy production is obtained with the $I_\infty = 15\%$-case if compared to the $I_\infty = 3\%$, both taken at their optimum. This is another confirmation, if needed, that ambient turbulence plays a major role on a tidal turbine farm energy production. Regarding the three C_P scenarios for the lower value of ambient turbulence, the *constant approach* only exhibits a small over-estimation of ≈ 0.7 GWh in the yearly energy production with respect to the two other scenarios, which perform similarly. However, this overestimation transcribed in the technico-economical assessment leads to a overestimation of nearly 26.5% in the profitability. This last result is far from negligible and highlights the need of accounting for the C_P modifications if one want to accurately model a tidal turbine energy production and profitability for any ambient turbulence level. Work still needs to be done to obtain an accurate description of the C_P modifications encountered by downstream turbine(s) for different inter-device distances, different ambient turbulence, lateral interactions, etc.

Acknowledgements

The authors would like to thank the Normandie regional council for its financial help in the framework of the *RHYNO* project, recently replaced by the *NEPTUNE* project. The authors also wish to thank the CRIANN for their available numerical computation resources and their useful expertise. This work received some support managed by the National Research Agency under the Investments for the Future programmes [ANR-10-IEED-0006-11]. Matías Fernández Hurst thanks the BEC-AR project for its financial and technical support during his stay in France. BEC-AR is an Argentinian government program that provides scholarship for training abroad in science and technology.

References

[1] U. Ahmed, I. Afgan, D. Apsley, T. Stallard, P. Stansby, Cfd simulations of full-scale tidal turbine: comparison of les and rans with field data, in: 11th European Wave and Tidal Energy Conference (EWTEC). Nantes, France.
[2] A.S. Bahaj, Generating electricity from the oceans, Renewable Sustainable Energy Rev. 15 (2011) 3399–3416.
[3] A.S. Bahaj, L. Myers, Analytical estimates of the energy yield potential from the alderney race (channel islands) using marine current energy converters, Renewable Energy 29 (2004) 1931–1945.
[4] T. Blackmore, W.M. Batten, A.S. Bahaj, Inlet grid-generated turbulence for large-eddy simulations, Int. J. Comput. Fluid Dyn. 27 (2013) 307–315.
[5] T. Blackmore, W.M. Batten, G.U. Műller, A.S. Bahaj, Influence of turbulence on the drag of solid discs and turbine simulators in a water current, Exp. Fluids 55 (2013).
[6] T. Blackmore, W.M.J. Batten, A.S. Bahaj, Influence of turbulence on the wake of a marine current turbine simulator, in: Proceedings of the Royal Society of London A: Mathematical, Physical and Engineering Sciences 470 (2014).
[7] T. Blackmore, B. Gaurier, L. Myers, G. Germain, A.S. Bahaj, The effect of freestream turbulence on tidal turbines, in: 11th European Wave and Tidal Energy Conference (EWTEC). Nantes, France.
[8] M.J. Churchfield, Y. Li, P.J. Moriarty, A large-eddy simulation study of wake propagation and power production in an array of tidal-current turbines, Philos. Trans. R. Soc. A: Math. Phys. Eng. Sci. 371 (2013).
[9] D.M. Culley, Tidal stream resource assessment through optimisation of array design with quantification of uncertainty, in: Proceedings of the 11th European Wave and Tidal Energy Conference.
[10] T. Divett, R. Vennell, C. Stevens, Optimization of multiple turbine arrays in a channel with tidally reversing flow by numerical modelling with adaptive mesh, Philos. Trans. R. Soc. A: Math. Phys. Eng. Sci. 371 (2013), pp.
[11] M. Edmunds, A. Williams, I. Masters, T. Croft, Bem-cfd: A reviesed model for accurate prediction, in: 11th European Wave and Tidal Energy Conference (EWTEC). Nantes, France.
[12] B. Elie, G. Oger, P.E. Guillerm, B. Alessandrini, Simulation of horizontal-axis tidal turbine wakes using a coupled approach with rankine-froude actuator disk model and a weakly-compressible finite volume solver, in: Proceedings of the ASME 32nd International Conference on Ocean, Offshore and Arctic Engineering (OMAE), ASME, 2013, pp. 1–5. Nantes, France.
[13] A.A. Environnementale, Projet Nepthyd, Technical Report, Conseil Général de l'environement et du développement durable: http://www.cgedd.developpement-durable.gouv.fr, last acces 2016, June the 16th.
[14] A.A. Environnementale, Projet Normandy Hydro, Technical Report, Conseil Général de l'environement et du développement durable: http://www.cgedd.developpement-durable.gouv.fr, last acces 2016, June the 16th.
[15] J.F. Filipot, M. Prevosto, C. Maisondieu, M.L. Boulluec, J. Thomson, Wave and turbulence measurements at a tidal energy site, in: Proceedings of 2015 IEEE/OES Eleventh Current, Waves and Turbulence Measurement Workshop (CWTM 2015).
[16] S.W. Funke, K.M. Thyng, T. Roc, Standard methodology for tidal array project optimisation: An idealized study of the minas passage, in: Proceedings of the 11th European Wave and Tidal Energy Conference.
[17] B. Gaurier, G. Germain, J. Facq, C. Johnstone, A. Grant, A. Day, E. Nixon, F.D. Felice, M. Costanzo, Tidal energy round robin tests comparisons between towing tank and circulating tank results, Int. J. Mar. Energy 12 (2015) 87–109, Special Issue on Marine Renewables Infrastructure Network.
[18] R. Karsten, A. Swan, J. Culina, Assessment of arrays of in-stream tidal turbines in the bay of fundy, Philos. Trans. R. Soc. A: Math. Phys. Eng. Sci. 371 (2013).
[19] S.C. Kramer, A continuous approach for the optimisation of tidal turbine farms, in: Proceedings of the 11th European Wave and Tidal Energy Conference.
[20] F. Lafon, G. Mattarolo, C.T. Pham, Hydrodynamic loads on paimpol-bréhat tidal current array export cable, in: 4th International Conference on Ocean Energy (ICOE). Dublin, Ireland.
[21] J. MacEnri, M. Reed, T. Thiringer, Influence of tidal parameters on seagen flicker performance, Philos. Trans. R. Soc. A: Math. Phys. Eng. Sci. 371 (2013).

[22] F. Maganga, G. Germain, J. Facq, B. Gaurier, E. Rivoalen, G. Pinon, Caractérisation expérimentale du sillage généré par une hydrolienne – influence du taux de turbulence ambiant, in: XIèmes Journées Nationales Génie Côtier / Génie Civil, Les Sables d'Olonne, France, pp. 795–802, doi:http://dx.doi.org/10.5150/jngcgc.2010.088-M, ISBN 978-2-35921-003-3.
[23] R. Malki, I. Masters, A. Williams, T. Croft, The influence on tidal stream turbine spacing on performance, in: 9th European Wave and Tidal Energy Conference (EWTEC). Southampton, UK.
[24] R. Malki, A. Williams, T. Croft, M. Togneri, I. Masters, A coupled blade element momentum – computational fluid dynamics model for evaluating tidal stream turbine performance, Appl. Math. Model. 37 (2013) 3006–3020.
[25] N. Maslov, J.F. Charpentier, C. Claramunt, A modelling approach for a cost-based evaluation of the energy produced by a marine energy farm, Int. J. Mar. Energy 9 (2015) 1–19.
[26] I. Masters, R. Malki, A.J. Williams, T.N. Croft, The influence of flow acceleration on tidal stream turbine wake dynamics: a numerical study using a coupled bem–cfd model, Appl. Math. Model. 37 (2013) 7905–7918.
[27] I.A. Milne, R.N. Sharma, R.G.J. Flay, S. Bickerton, Characteristics of the turbulence in the flow at a tidal stream power site, Philos. Trans. R. Soc. A: Math. Phys. Eng. Sci. 371 (2013).
[28] P. Mycek, B. Gaurier, G. Germain, G. Pinon, Élie Rivoalen, Numerical and experimental study of the interaction between two marine current turbines, in: 9th European Wave and Tidal Energy Conference (EWTEC). Southampton, UK.
[29] P. Mycek, B. Gaurier, G. Germain, G. Pinon, E. Rivoalen, Numerical and experimental study of the interaction between two marine current turbines, Int. J. Mar. Energy 1 (2013) 70–83.
[30] P. Mycek, B. Gaurier, G. Germain, G. Pinon, E. Rivoalen, Experimental study of the turbulence intensity effects on marine current turbines behaviour. part I: One single turbine, Renewable Energy 66 (2014) 729–746.
[31] P. Mycek, B. Gaurier, G. Germain, G. Pinon, E. Rivoalen, Experimental study of the turbulence intensity effects on marine current turbines behaviour. part II: two interacting turbines, Renewable Energy 68 (2014) 876–892.
[32] L. Myers, K. Shah, P. Galloway, Design, commissioning and performance of a device to vary the turbulence in a recirculating flume, in: 10th European Wave and Tidal Energy Conference.
[33] S.P. Neill, E.J. Litt, S.J. Couch, A.G. Davies, The impact of tidal stream turbines on large-scale sediment dynamics, Renewable Energy 34 (2009) 2803–2812.
[34] D. O'Doherty, A. Mason-Jones, C. Morris, T. O'Doherty, C. Byrne, P. Prickett, R. Grosvenor, Interactions of marine turbines in close proximity, in: 9th European Wave and Tidal Energy Conference (EWTEC). Southampton, UK.
[35] E. Osalusi, J. Side, R. Harris, Reynolds stress and turbulence estimates in bottom boundary layer of fall of warness, Int. Commun. Heat Mass Transfer 36 (2009) 412–421.
[36] E. Osalusi, J. Side, R. Harris, Structure of turbulent flow in emec's tidal energy test site, Int. Commun. Heat Mass Transfer 36 (2009) 422–431.
[37] C. Peyrard, C. Buvat, F. Lafon, C. Abonnel, Investigations of the wake effects in marine current farms, through numerical modelling with the telemac system, in: 1st International Conference on Ocean Energy (ICOE). Bremerhaven, Germany.
[38] Previmer, Previmer data base: http://www.previmer.org/, last acces 2016, June the 16th.
[39] T. Roc, D.C. Conley, D. Greaves, Methodology for tidal turbine representation in ocean circulation model, Renewable Energy 51 (2013) 448–464.
[40] T. Stallard, R. Collings, T. Feng, J. Whelan, Interactions between tidal turbine wakes: experimental study of a group of three-bladed rotors, Philos. Trans. R. Soc. A: Math. Phys. Eng. Sci. 371 (2013).
[41] J. Thiébot, P.B. du Bois, S. Guillou, Numerical modeling of the effect of tidal stream turbines on the hydrodynamics and the sediment transport – application to the alderney race (raz blanchard), france, Renewable Energy 75 (2015) 356–365.
[42] J. Thomson, B. Polagye, V. Durgesh, M. Richmond, Measurements of turbulence at two tidal energy sites in Puget Sound, WA, IEEE J. Oceanic Eng. 37 (2012) 363–374.
[43] J. Thomson, B. Polagye, M. Richmond, V. Durgesh, Quantifying turbulence for tidal power applications, Oceans (2010) 1–8.
[44] M. Togneri, I. Masters, Synthetic turbulence generation for turbine modelling with BEMT, in: 3rd Oxford Tidal Energy Workshop, Oxford, UK.
[45] R. Vennell, A. Harang, M. Smeaton, M. Gerritsen, Giga watt arrays: How many tidal turbines will it take?, in: Proceedings of the 11th European Wave and Tidal Energy Conference.